Journal of Food Engineering 150 (2015) 106–116

Contents lists available at ScienceDirect

Journal of Food Engineering

journal homepage: www.elsevier.com/locate/jfoodeng

A new methodology to estimate the steady-state permeability of roast and ground coffee in packed beds

B.R. Corrochano [a,b,*], J.R. Melrose [b], A.C. Bentley [b], P.J. Fryer [a], S. Bakalis [a]

[a] Centre for Formulation Engineering, Department of Chemical Engineering, University of Birmingham, Edgbaston, Birmingham B15 2TT, UK
[b] Mondelēz International, Coffee Global Centre of Excellence, Ruscote Avenue, Banbury OX16 2QU, UK

ARTICLE INFO

Article history:
Received 10 February 2014
Received in revised form 2 November 2014
Accepted 15 November 2014
Available online 22 November 2014

Keywords:
Coffee extraction
Espresso coffee
Under/over extraction
Packed bed
Permeability

ABSTRACT

In an espresso-style extraction hot water (90 ± 5 °C) is driven through a coffee packed bed by a pressure gradient to extract soluble material from the coffee matrix. Permeability is a key parameter affecting extraction as it determines the flow rate through the bed and hence brewing and residence time. This may alter bed-to-cup mass transfer and therefore impact brew quality.

In this work a methodology that will allow estimation of the permeability of coffee packed beds in steady-state was developed. Fitting measured flow rate – pressure drop data to Darcy's law resulted in permeability values in the range of 10^{-13}–10^{-14} m^2. Disagreement between the experimental and theoretical permeability, as estimated from dry measurements of particle size distribution and Kozeny–Carman equation, was found. Bed consolidation may have a larger effect on the packing structure than the mere decrease in bed bulk porosity. The Kozeny–Carman equation, corrected with a porosity-dependent tortuosity according to a power law, gave a good fit of the data.

1. Introduction

According to the International Coffee Organisation (2013), approximately 1.6 billions cups of coffee are consumed worldwide everyday, making coffee beans one of the most-traded commodities. The most popular brewing methods require a pressure gradient to drive hot water (90 ± 5 °C) through a packed bed of roasted and ground coffee to extract soluble material from the coffee matrix (Petracco, 2001). This is the case of Italian espresso, novel On-Demand capsule systems (pre-portioned capsules of roast and ground coffee that are brewed using a small automatic brewer) or, at an industrial scale, instant coffee production. In the latter process extraction temperatures as high as 180 °C are used (Clarke, 2001).

Significant effort has been devoted to optimise espresso-style coffee extraction variables to meet consumers' taste. An extraction yield, defined as the mass percentage of roast and ground coffee dissolved in the brew, between 18% and 22% has been proposed as acceptable in terms of brew quality (Navarini et al., 2009). Romani et al. (2004) found in a field study across Italian coffee shops that between 6 and 9 g of ground coffee are typically used in espresso-style extraction; average drink volume and extraction yields were around 22 ml and 24%, respectively. Poor quality in espresso brews is commonly attributed to under and over-extraction. Although the definition of these phenomena may be somewhat subjective, they have been characterised, from a sensory point of view, by low extraction yields with an acid, sweet flavour profiles and high extraction yields with a bitter, astringent flavour profile, respectively (Petracco, 2001).

The influence of product formulation (i.e. botanical kind of the beans, roasting degree, and particle size distribution) and process variables (i.e. extraction time, flow rate, temperature and water pressure) on the physicochemical attributes and sensory profile of espresso brews have been widely studied, such as by Andueza et al. (2002, 2003, 2007), Caprioli et al. (2012), Gloess et al. (2013), Lindinger et al. (2008), Maeztu et al. (2001) and Parenti et al. (2014). Although relevant conclusions may be drawn from these studies (e.g. high temperatures and fine particle size distributions may lead to over-extracted brews) it is also true that the lack of a more engineering approach to the physical mechanism driving the process has promoted some misconceptions and myths surrounding coffee extraction. This is especially true when the role of hydrodynamics process variables is discussed; their dependency on other variables is subtle and is sometimes neglected. For example, Andueza et al. (2002) studied 'water pressure' as a variable that may affect the quality of espresso brews, but they implicitly

* Corresponding author at: School of Chemical Engineering, University of Birmingham, Edgbaston, Birmingham, West Midlands B15 2TT, UK. Tel.: +44 7446 035153.
E-mail address: bxr008@bham.ac.uk (B.R. Corrochano).

http://dx.doi.org/10.1016/j.jfoodeng.2014.11.006
0260-8774/

considered it to be independent of particle size distribution, packed bed structure, and flow rate.

In regard to the influence of hydrodynamics in the final quality of espresso coffee, the permeability of the packed beds is a key parameter. For a fixed pressure gradient, the permeability determines the flow rate across the bed and hence brewing time (i.e. time required to produce a given drink volume) and water residence time; the influence of short or long contact times on mass transfer can lead to under or over extracted brews. Therefore there is a genuine motivation to develop predictive models to estimate the permeability of coffee packed beds.

For low Reynolds numbers ($Re_p < 10$) and steady-state, the permeability can be estimated from Darcy's law (Bear, 1988):

$$Q = \frac{KA}{\mu L}\Delta P \tag{1}$$

where Q is the volumetric flow rate, A the cross section area normal to the flow direction, ΔP the pressure drop across the bed, μ the fluid viscosity, L the length of the bed and K the permeability of the medium. In a packed bed the relevant length scale to calculate Reynolds number is an estimation of the equivalent pore size of the bed (Rhodes, 2008).

Petracco and Liverani (1993), based on the following observations, stated that espresso-style extraction takes place during the transient regime of the flow: (i) during the first 2–3 s of extraction, flow rapidly increased and then exponentially decreased by 60–85%; (ii) average flow rate increased as average extraction temperature decreases; (iii) increasing the pressure head above a certain point (~5–7 bar) was found to decrease the average flow rate. The latter observation has also been reported in chromatography studies and was attributed to bed consolidation (Hekmat et al., 2011). Furthermore, in hydration experiments of coffee particles in a beaker, Mateus and Rouvet (2007) reported a dynamic swelling effect due to moisture absorption by the cellulose matrix. Despite the aforementioned non-steady state observations, permeability values have been estimated using Eq. (1). In works concerned with the use of stove-top coffee makers, King (2008) found values of fluid conductance, α, (defined as the proportionality factor between the applied pressure across the bed and the volumetric flow rate) of 1.00×10^{-10} m^3 Pa^{-1} s^{-1}, which is equivalent to a permeability value of 8.98×10^{-13} m^2. This is in good agreement with Navarini et al. (2009), who derived a time-dependent permeability ranging from 7.00×10^{-14} to 4.00×10^{-13} m^2, but is significantly different from Gianino (2007), who reported a value of 2.3×10^{-12} m^2.

Permeability is an exclusive function of particle size distribution of the solids forming the bed and packing structure (i.e. bed bulk porosity). Although this dependency has been thoroughly investigated in many industrial applications, such as chromatography (Hekmat et al., 2011), filtration (Tien and Ramarao, 2013), and oil-containing geological formations (Joseph et al., 2013), to the best of our knowledge, no work has been reported before for coffee packed beds. Therefore the main objectives of this work are to (i) develop a methodology to estimate the permeability of roast and ground coffee packed beds in steady-state and (ii) evaluate and model the effect of particle size distribution and bed bulk porosity (effectively bed bulk density) on permeability.

2. Permeability models

A common modelling approach is to portray the bed as a bundle of parallel capillaries in which the Hagen-Poiseuille equation is applied. The implicit assumption of a homogenous bed (i.e. wall effect can be neglected) remains true for bed-particle diameter ratios $\geqslant 5$ (Di Felice and Gibilaro, 2004). The general expression resulting from this approach (assuming that capillaries are cylindrical) is given in Eq. (2). A detailed derivation can be found elsewhere (Endo et al., 2002; Rhodes, 2008):

$$K = \frac{\varepsilon_{bed}^3}{2\tau^2 S_v^2 (1-\varepsilon_{bed})^2} \tag{2}$$

where ε_{bed} is the average bulk porosity of the packed bed, S_v the surface-to-volume ratio of the packing material and τ the tortuosity of the bed; τ is defined as the ratio of the actual tortuous length travelled by the fluid in the bed to the geometric length of the bed.

The simplest case, where the packing material is formed by mono-sized spheres, implies that $S_v = 6/d_s$ and $\tau = 1.58$; Eq. (2) is then reduced to Eq. (3), known as the Kozeny–Carman equation:

$$K = \frac{\varepsilon_{bed}^3 d_s^2}{180(1-\varepsilon_{bed})^2} \tag{3}$$

where d_s is the diameter of the packing spheres and 180 the Kozeny–Carman pre-factor. If the packing material is non-spherical and exhibits a distribution of sizes, this must be taken into account as $d_s = \Phi d_{[3,2]}$, where Φ is the sphericity of the material and $d_{[3,2]}$ is the average Sauter mean diameter of the distribution. Eq. (3), combined with Eq. (1), has been proved to make reasonable estimates of pressure drops (errors of ±50%) for unconsolidated beds in the range of ε_{bed} from 0.36 to 0.92 (Macdonald et al., 1979). However, as reported in the same work, when the beds strongly deviated from Kozeny–Carman assumptions, (i.e. consolidated beds with ε_{bed} considerably lower than the theoretical 0.36 found by Scott (1960) for random closed packed beds of mono-sized spheres), estimation errors in the pressure drop of up to 300% were found. This suggests that tortuosity, assumed to be constant in Eq. (3), is notably affected by consolidation of the bed. Tortuosity-bed bulk porosity relationships have been thus investigated. For example, Lanfrey et al. (2010) modelled tortuosity of an isotropic packed bed as a decreasing function of bed bulk porosity. However, commercially-available ground coffee has been reported to be characteristically bimodal (Petracco, 2005). A semi-empirical tortuosity-bed bulk porosity correlation for beds formed by a discrete bimodal distribution of spheres has been reported by Dias et al. (2006):

$$\tau = \left(\frac{1}{\varepsilon_{bed}}\right)^n \tag{4}$$

where n is an adjustable parameter which depends on the packing method and varies from 0.4, for loose packed beds, to 0.5, for dense packed beds of spheres.

Two different models will be then considered to estimate the permeability of coffee packed beds: Model 1 (Kozeny–Carman equation, Eq. (5a)) and Model 2 (Kozeny–Carman with a porosity-dependent tortuosity, Eq. (5b)), obtained by substituting Eq. (4) in Eq. (2):

$$K = \frac{\varepsilon_{bed}^3 (\phi d_{[3,2]})^2}{180(1-\varepsilon_{bed})^2} \tag{5a}$$

$$K = \frac{\varepsilon_{bed}^3 (\phi d_{[3,2]})^2}{72\left(\left(\frac{1}{\varepsilon_{bed}}\right)^n\right)^2 (1-\varepsilon_{bed})^2} \tag{5b}$$

3. Materials and methods

3.1. Extraction rig

A rig (Fig. 1) was designed and built to carry out fixed-time brewing cycles. Two main sections are to be distinguished:

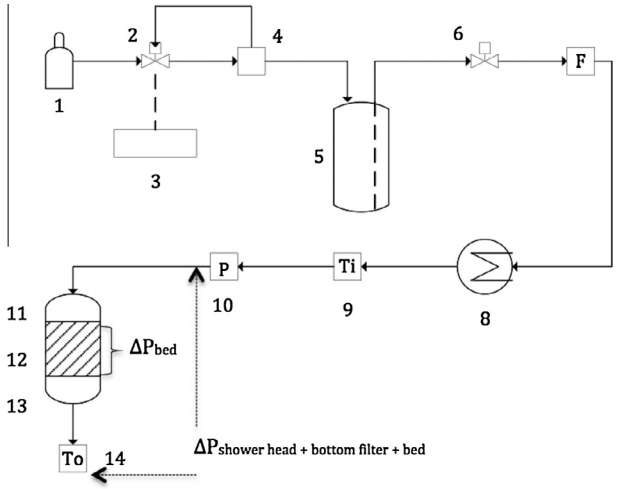

Fig. 1. Extraction rig; (1) compressed air source; (2) electro-pneumatic valve; (3) power supply for electro-pneumatic valve; (4) regulator; (5) keg-like water tank; (6) valve; (7) flow meter; (8) boilers; (9) inlet thermocouple; (10) pressure transducer; (11) shower head distributor; (12) brewing chamber (containing the packed bed); (13) bottom filter; (14) outlet thermocouple.

Extraction section: To simulate the filter basket geometry of traditional espresso machines, an extraction cell of diameter–length (D/L) ratio of 2 was built by assembling together three independent pieces: (i) a bottom filter; (ii) a brewing chamber containing the coffee packed bed (volume = 2.00×10^{-5} m^3, $D = 3.70 \times 10^{-2}$ m, $L = 1.85 \times 10^{-2}$ m); and (iii) a shower head distributor. The temperature before and after the extraction section was measured by two thermocouples. The pressure drop across the packed bed was estimated from the measurement provided by the pressure transducer located before the extraction cell; the hydraulic resistances of the shower head distributor and the bottom filter, which had been previously measured, were subtracted from the measurement.

Pumping and heating section: A cylindrical keg-like water tank, with two pipe connection points at the top (IMI Cornelius, UK), was connected to a compressed air source (maximum pressure 6.00×10^5 Pa). The aperture of an electro-pneumatic valve (ITV2050-31F2BS3, SMC, USA) set the magnitude of the hydrostatic pressure achieved inside the tank and kept it constant. The brewing cycle started when the timed-valve (UDT Timer, Tempatron, UK) was opened. Flow rate was measured by means of an ultrasonic flow meter located after the tank (USC-731, Malema, USA). The measured variables were continuously recorded (10 measurements per second) with the aid of a custom data logging system. Software to operate the rig was developed with LabView (National Instrument, Germany).

3.2. Roast and ground coffee

Medium-dark roasted arabica beans from Central America and Brazil (moisture content <5%) were ground in a Dalla Corte grinder (Baranzate, Italy) to produce four different particle size distributions, A–D. The particle size distributions were measured using laser diffraction (Helos, Sympatec, UK); the sphericity of the particles was estimated with an image analyser (QICPIC, Sympatec, UK). For both parameters three independent samples of approximately 10–20 g from each particle size distribution, A–D, were measured, using air as a dry disperser, and the results averaged.

Although particle size distributions can alternatively be assessed using a liquid as a disperser (wet measurement), and generally the results differ, theoretical modelling based on dry measurements is investigated in this work since they are the typical (and practical) measurement performed at manufacturing sites.

3.3. Packed beds

Each particle size distribution, A–D, was prepared in three beds of different weights, 7.2×10^{-3}, 8.0×10^{-3} and 9.5×10^{-3} kg, respectively. The beds were tapped 100 times to create a homogeneous distribution of the particles. Coffee was axially compressed afterwards with a tamper, reducing its volume until the volume of the brewing chamber was matched. Initial bed bulk densities of 360, 400 and 480 kg m^{-3} were achieved; all the beds were produced in triplicate. The applied force to pack the beds to the final density was estimated with an axial compression test carried out in a Z030 mechanical tester (Zwick/Roell, UK) at a compression rate of 0.1 mm s^{-1} and maximum force of 300 N.

3.4. Intrinsic solid density of roasted coffee, particle porosity and bed bulk porosity evaluation

The bed bulk density is related to bed bulk porosity as follows:

$$\rho_{\text{bulk}} = \rho_{\text{particle}}(1 - \varepsilon_{\text{bed}}) \tag{6a}$$

where ρ_{bulk} is the bed bulk density, ρ_{particle} the particle density of roasted coffee, and ε_{bed} the bed bulk porosity.

A roast coffee bean is a porous material (Schenker et al., 2000); it consists of nano-porous cell walls and larger cell pockets (25–40 μm), which contained the original biological cell before roasting. Thus the particle density of roasted coffee was estimated using Eq. (6b):

$$\rho_{\text{particle}} = \rho_{\text{solid}}(1 - \varepsilon_{\text{particle}}) \tag{6b}$$

where ρ_{solid} is the intrinsic solid density of roasted coffee, defined as mass of coffee divided by its solid matrix volume, and $\varepsilon_{\text{particle}}$ the porosity of the particles. The latter was estimated as the contribution of closed porosity, defined as the volume percentage of a particle which is occupied by isolated pores, and open porosity, defined as the volume percentage of a particle occupied by an interconnected network of pores reachable from the outside.

The intrinsic specific solid volume (reciprocal of the intrinsic solid density) and the specific volume of closed pores were measured with Helium pycnometry (AccuPyc II 1340 Helium Pycnometer, Micromeritics). As reported by Mateus and Rouvet (2007), a very fine distribution (average particle size of $d_{[3,2]} = 48.12 \times 10^{-6}$ m in this work) was used to determine the intrinsic specific solid volume. The underlying assumption is that closed porosity is attributed to intact cell pockets (*circa* 25–40 μm, as reported by Schenker et al., 2000) within the structure of the grain; thus in a particle size in the same range of magnitude of the intact cell pockets, the presence of closed pores is highly unlikely. The specific volume of closed pores was estimated by subtracting the specific solid volume (as previously determined) from the measured specific volume of the considered distribution. For all the measurements, between 0.1500 and 0.2500 g were measured in an electronic balance with an accuracy of 10^{-4} g, and then placed into the pycnometer chamber. Air was evacuated in 50 purges cycles and 10 measurements of the solid volume were performed.

The specific volume of open pores was measured by mercury porosimetry (AutoPore IV 9500 Mercury Porosimeter, Micromeritics). Between 0.2000 and 0.3500 g were measured using an electronic balance with an accuracy of 10^{-4} g, and then transferred into a cylindrical penetrometer suitable for powder samples. Mercury was fed to the penetrometer at progressively increasing

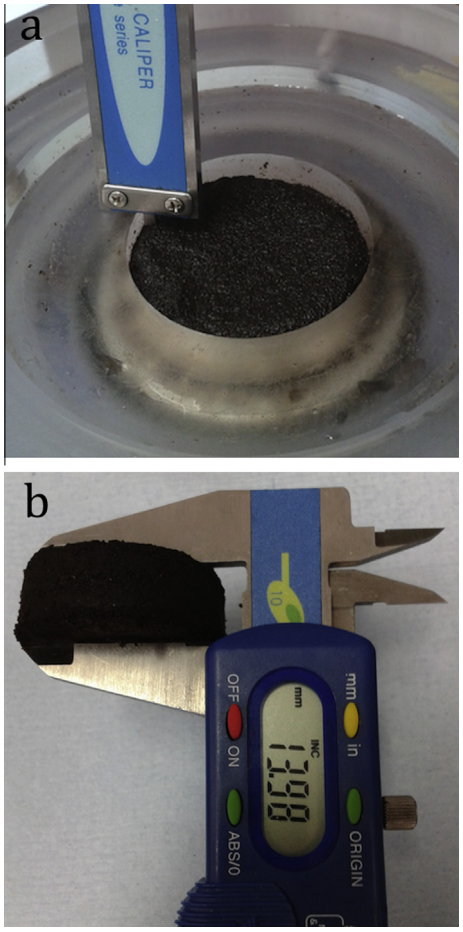

Fig. 2. (a) Measurement of the height reduction (L_t) at a given time point; (b) measurement of the actual height of the bed (L_{actual}) after 600 s.

pressures (from 0 to approximately 2×10^8 Pa). The pore size distribution was estimated by:

$$d_{pore} = -\frac{4\varphi}{P}\cos\theta \quad (7)$$

where d_{pore} is pore diameter, P is the applied pressure, γ is the surface tension of Hg (0.485 N m^{-1} at 25 °C), and θ is the contact angle between the Hg and the porous solid; although the contact angle value depends on the solid surface and values between 128° and 148° have been previously reported, a typical value of 130°, common in most practical applications, has been assumed in this work out of convenience (Giesche, 2006).

Table 1
Average particle size ($d_{[3,2]}$) of the four considered particle size distributions measured by laser diffraction using air as dry disperser ± standard deviation of the measurement of three independent samples of each distribution.

Particle size distribution	$d_{[3,2]}$ (m)
A	$79.73 \pm 0.48 \times 10^{-6}$
B	$101.60 \pm 0.20 \times 10^{-6}$
C	$112.86 \pm 1.08 \times 10^{-6}$
D	$131.36 \pm 2.06 \times 10^{-6}$

To determine the volume of mercury filling the penetrometer, and therefore not representing the open porosity within the particles, it was assumed that greatest pore size that would be present within a particle was ~40 μm, based on the previous assumption of the size of the cell pocket. From Eq. (7), the applied pressure corresponding to this pore size was estimated and was considered as the initial point in which mercury would start penetrating into the pores of the particles.

All the measurements were carried out on three independent samples of each of the four particle size distributions, A–D, and the results were averaged.

3.5. Bed hydration and flow rate – pressure drop data collection

To achieve steady-state water was circulated through the extraction cell for 600 s. By this time coffee grains were fully extracted, and therefore the results reported here are for extracted beds. Typical temperatures for coffee extraction (i.e. 90 ± 5 °C) are commonly measured in the boiler of the coffee machine and, as a result of heat losses, lower effective extraction temperatures are actually used. Thus an average temperature of 80 °C was used for all the experiments.

Preliminary experiments showed that the hydration conditions must be carefully chosen to avoid physical damage on the structure of the bed which can lead to undesirable effects, such as macro-channelling. Hydrostatic pressures in the tank were selected according to the initial bed bulk density of the packed beds and were 2.50, 3.00 and 4.50×10^5 Pa for initial bed bulk density of 360, 400 and 480 kg m^{-3}, respectively.

At the steady-state experimental flow rate-pressure drop data was collected. The hydrostatic pressure in the tank was varied from 4.5×10^5 Pa to 0.5×10^5 Pa in steps of 0.5×10^5 Pa. At each step, the instant values of flow rate and pressure drop across the bed were recorded during 60 s for subsequent processing.

3.6. Bed consolidation

It was observed that, upon application of flow, the beds consolidated. The initial bed height decreased and ground coffee evolved

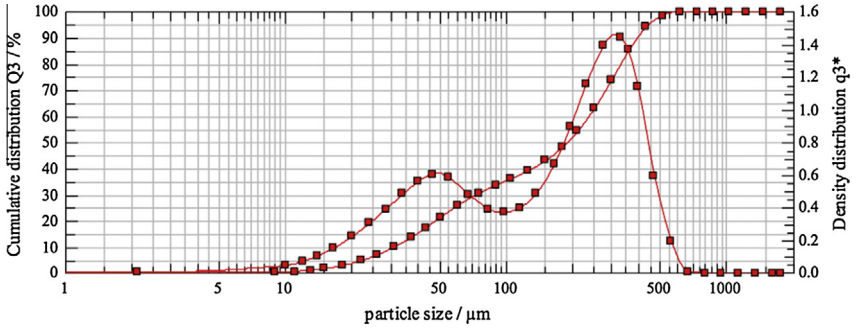

Fig. 3. Probability density distribution (right y-axis, bi-modal curve) and cumulative volume distribution (left y-axis) obtained for particle size distribution A. The x-axis represents the particle size (μm) in logarithmic scale.

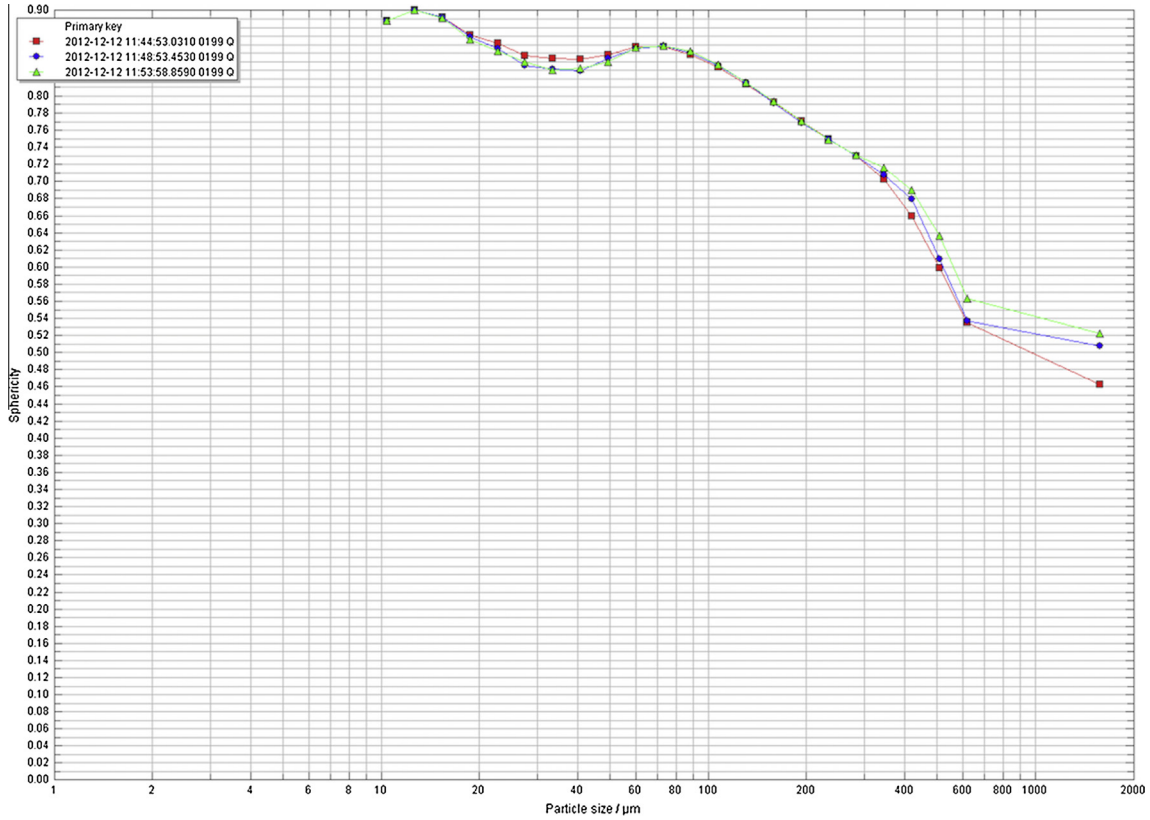

Fig. 4. Particle sphericity (*y*-axis) of three independent samples of particle size distribution A. The particle size (μm) is shown in the *x*-axis in logarithmic scale.

to be an agglomeration of particles. Dynamic bed consolidation was determined in an independent experiment replicating the hydration procedure described in Section 3.5. At different time points bed height reduction was measured as shown in Fig. 2a and the consolidation degree calculated from Eq. (8a):

$$\lambda(t)_{\text{depth}} = \frac{L_t}{L_0} \tag{8a}$$

where L_0 is the initial bed height and L_t the bed height reduction at each time point.

To ensure that the bed did not further consolidate during the steady-state experiments, after the last measurement at 600 s, the hydrostatic pressure in the water tank was increased to the maximum pressure (4.5×10^5 Pa) during 60 s, and an additional measurement of the height was taken. The coffee bed was then carefully removed from the brewing chamber and the actual height measured (Fig. 2b). The consolidation degree was also calculated from this measurement according to Eq. (8b):

$$\lambda(t_{600})_{\text{length}} = \frac{L_0 - L_{\text{actual}}}{L_0} \tag{8b}$$

where L_{actual} is the measured bed height.

The average steady-state consolidation degree was calculated as follows:

$$\lambda_{\text{average}} = \frac{\lambda(t_{600})_{\text{depth}} + \lambda(t_{600})_{\text{length}}}{2} \tag{8c}$$

The steady-state bed bulk porosity, when the bed was fully consolidated, was calculated accounting for consolidation as reported by Hekmat et al. (2011):

$$\varepsilon_{ss} = \frac{\varepsilon_{\text{bed}} - \lambda_{\text{average}}}{1 - \lambda_{\text{average}}} \tag{9}$$

where ε_{ss} is the bed bulk porosity of the fully consolidated bed and ε_{bed} the initial bulk porosity of the bed as calculated from Eq. (6a).

4. Results and discussion

4.1. Particle size distribution characterisation

All the particle size distributions, A–D, were found to be characteristically bimodal. Fig. 3 shows a typical result in which the probability density distribution and the cumulative volume distribution obtained for particle size distribution A are displayed. The fine peak was invariably located around 40–50 μm for all the distributions, whereas the coarse peak shifted when coarser distributions were obtained. The fine and coarse particle volume percentages, given by the cumulative volume distribution, also varied; the former decreased when coarser distributions were obtained. Table 1 shows the resulting $d_{[3,2]}$ of the four considered distributions.

Fig. 4 shows a typical example of sphericity measurement of three independent samples of particle size distribution A; similar results were obtained for the rest of the particle size distributions, B–D. The sphericity ranged in all particle size distributions from 0.90 for the fine particles in the distribution (~20 μm) to 0.52–0.73 for the coarser particles (~600 μm). The last sphericity point, always corresponding to particle sizes of 1000–2000 μm, was neglected as this might correspond to lumps of material not properly dispersed; size distribution measurements performed with the reference dry method (as described in Section 3.2) shows that in particle size distribution A the biggest particle size is around 500 μm (Fig. 3). The mean sphericity for the particle size distributions was then estimated to be between 0.71 and 0.80; since the assessment method is of approximate nature, the average value of the four mean sphericity, 0.75, was adopted as representative for all the particle size distributions, A–D.

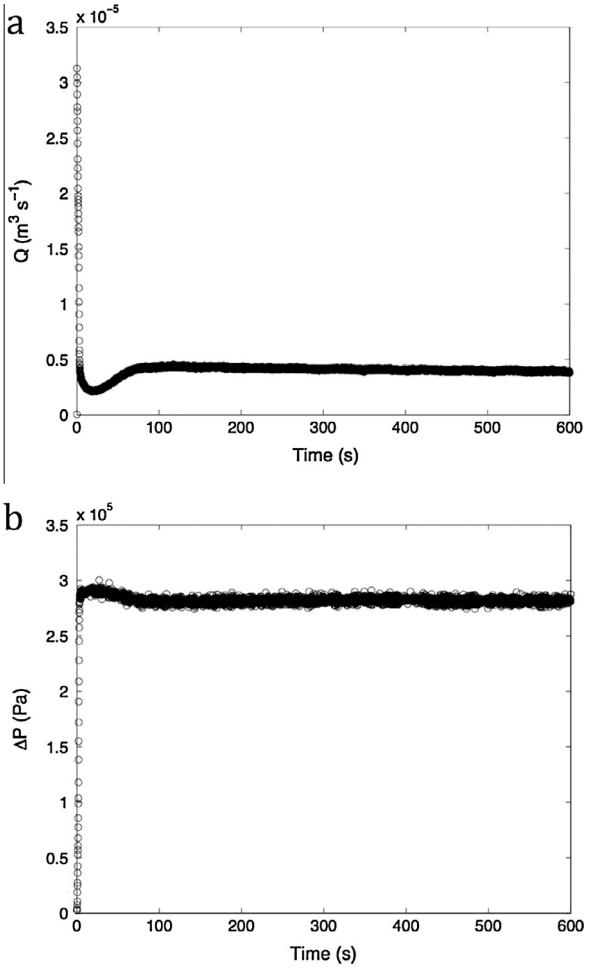

Fig. 5. Transient profiles during the hydration of a packed bed of particle size distribution A at an initial bed bulk density of 400 kg m^{-3}; (a) flow rate (Q); (b) pressure drop (ΔP).

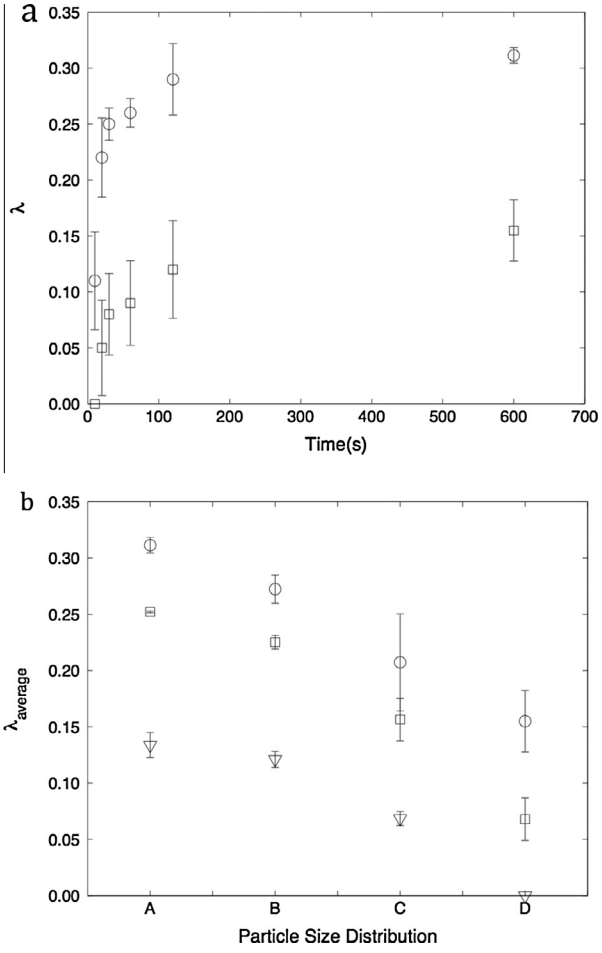

Fig. 6. (a) Consolidation rate as calculated with Eq. (8a) for particle size distribution A (○) and particle size distribution D (□) with a starting bed bulk density of 360 kg m^{-3}; (b) average steady-state consolidation degree after 600s as calculated with Eq. (8c), at the starting bed bulk density of 360 kg m^{-3} (○), 400 kg m^{-3} (□) and 480 kg m^{-3} (▽). The error bars represent the standard deviation of the measurement on three independent beds of each particle size distribution.

4.2. Transient regime

A transient regime was found during the first 60–80 s of the operation. Fig. 5a and b shows the typical flow rate and pressure drop profile during the hydration stage. The maximum in Fig. 5a corresponds to the sudden opening of the timed-valve of the tank and the filling of the hydraulic circuit before the bed. As the wetting front travels through the bed, the flow rate decreases due to the bed resistance increasing with length of bed already penetrated. Once the bed is filled the flow then increases over the next 60–80 s before reaching the quasi steady-state. The observed behaviour was very similar to the one presented here. Measurements of the permeability discussed in the next sections were taken after this time.

In general, the qualitative observations on the transient flow agree with the literature (Petracco and Liverani, 1993). They reported effects on reversing the direction of the flow through a coffee packed bed. They interpret the reappearance of the transient flow as due to fines particles migration. However, we believe that these transient effects are just the hydraulic circuit before the extraction chamber being re-filled (flow rate rises to a peak) and a new front moving through the bed (flow rate decreases).

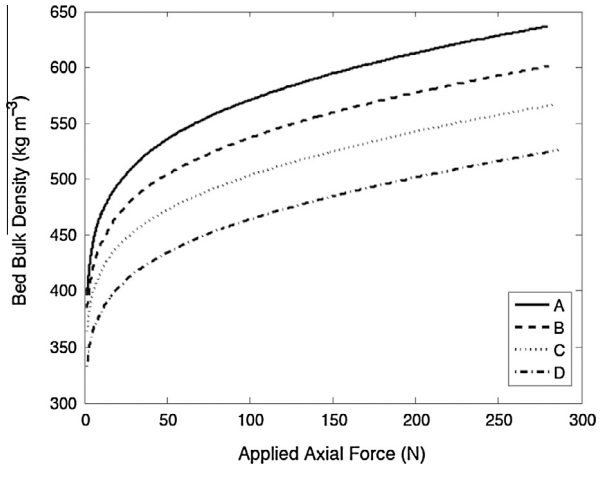

Fig. 7. Bed bulk density evolution (y-axis) as a function of the applied axial force on the packed beds (x-axis) for the four considered particle size distributions (A-D).

4.3. Bed consolidation

The consolidation rate of the bed, calculated with Eq. (8a), was found to be exponential and occurred predominately within the first 30–60 s of applied flow (Fig. 6a); after 600 s the bed was fully consolidated. The steady-state consolidation degree, as calculated with Eq. (8c), varied from 0% (distribution D with an initial bed bulk density of 480 kg m^{-3}) to 31% (distribution A with an initial

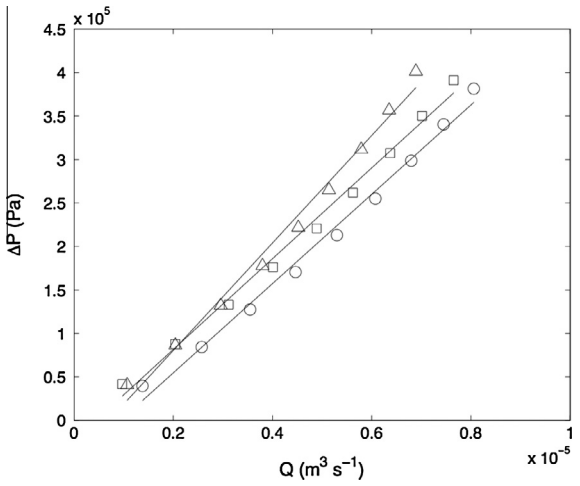

Fig. 8. Flow rate (*x*-axis) –pressure drop (*y*-axis) for three independent samples of particle size distribution A at the starting bed bulk density of 360 kg m^{-3}. The solid lines represent the best-fit lines ($R^2 > 0.97$ for all cases) from the data to Eq. (1), rearranged to make *Q* the independent variable. Permeability values were derived from each of the data set and subsequently averaged.

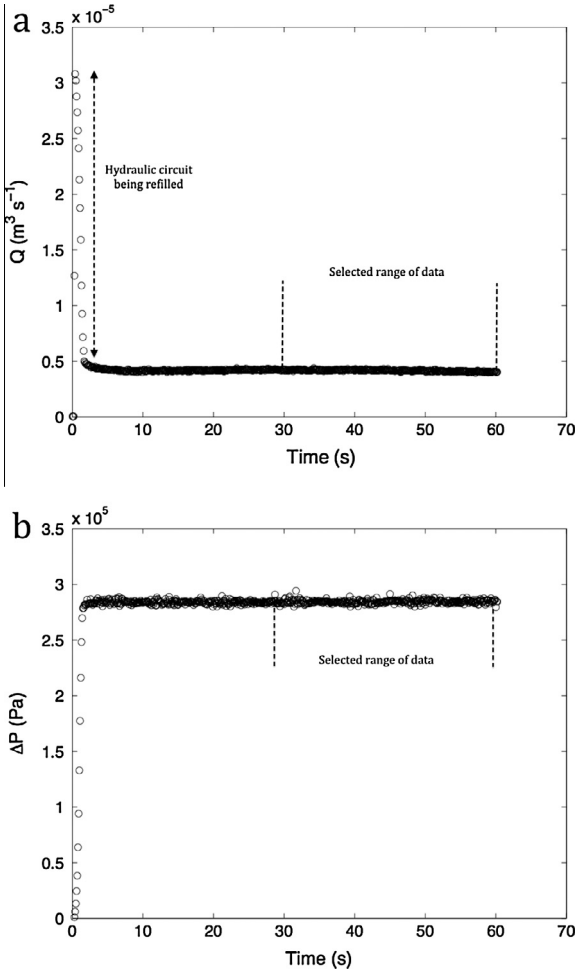

Fig. 9. Collection of experimental data after bed hydration; (a) flow rate (*Q*); (b) pressure drop (Δ*P*). This particular example corresponds to one of the three repetitions of the sixth flow rate-pressure drop point (from bottom to the top) in Fig. 10b for particle size distribution A (○). This resulting point is the average of the selected range of data showed here.

bed bulk density of 360 kg m^{-3}) (Fig. 6b). In general, the coarser the distribution the less consolidation experienced under flow. This is consistent with the higher axial forces applied on coarser distributions during packing, as estimated with the axial compression test (Fig. 7); these higher forces produce beds that are more stable under flow. In addition the measured axial forces were comparable to the range ('few kilos' to 20 kgf) reported by Petracco (2005) for espresso-style extraction.

4.4. Steady-state permeability

Estimations of Re_p for the considered experimental conditions were between 0.04 and 4; this confirms that the flow through our beds is laminar ($Re_p \geqslant 10$ for turbulent flow) and thus the Darcy equation can be used. Fig. 8 shows an example of the best fit lines of experimental steady-state flow rate-pressure drop across the bed to Darcy's equation (i.e. Eq. (1) with *Q* as the independent variable); the data was collected from three independent samples of particle size distribution A at $\rho_{bed} = 360$ kg m^{-3}. All the linear regressions showed a $R^2 > 0.97$. Three permeability values were calculated and subsequently averaged. Each individual experimental point shown in Fig. 8 corresponds to the average of the flow rate-pressure drop points of the last 30 s of each experiment (described in Section 3.5), which lasted 60 s. Fig. 9a and b shows an example of the collected data that was subsequently averaged to produce one of the points showed in Fig. 8. As shown in Fig. 9, after the 2–3 first seconds (when the hydraulic circuit before the extraction chamber was being refilled), the system reaches steady-state. For the sake of clarity, the experimental steady-state flow rate-pressure drop data collected in the measurements performed on the three individual samples of each particle size distribution is shown in Fig. 10a–c as averages rather than as three individual data sets as in Fig. 8.

The derived permeability values (Table 2) lie between 3.36×10^{-13} and 2.59×10^{-14} m^2 and are in good agreement with those presented in Section 1 (4.00×10^{-13}–7.00×10^{-14} m^2, reported by King (2008) and Navarini et al. (2009)). As acknowledged by Navarini et al., the permeability values reported by Gianino (2007) are underestimated. An analysis of variance (ANOVA) was performed where the sources of variation were the particle size distribution and the bulk bed density. A Tukey *T*-test was subsequently performed (risk level, $\alpha = 0.05$). The statistical analysis was conducted in JMP 11® (SAS Institute, USA). As one can see in Table 2, the estimated permeability values are overall significantly different across the tested particle size distributions and bed bulk density values. However, for particle size distribution B and C there is no significant difference at $\rho_{bulk} = 360$ kg m^{-3} and 400 kg m^{-3}; this could be due to the bed consolidation resulting in very similar packed beds in the steady-state.

Across the whole range of data, the greatest to the smallest permeability ratio is 17. This is a significant variance, especially when the implications in coffee extraction are considered: for a fixed pressure head given by a coffee machine pump, the obtained flow rate would be 17 times higher comparing the lowest and highest permeability. In a modern On-Demand system, variation of the permeability of the bed moves the operating point of the pump along the pump characteristic curve (e.g. low permeability beds lead to high pressures and low flow rates). It is also well known by coffee baristas that the selection of a coarse/fine particle size distribution and the packing of the bed can lead to under/over-extraction (Andueza et al., 2007); it is likely that these phenomena are mainly driven by permeability altering flow rate (i.e. brewing and residence time) and thus mass transfer.

The data also confirms the extreme sensitivity of permeability to bed bulk density (i.e. bed bulk porosity). An increment in the initial bed bulk density of approximately 30% (360–480 kg m^{-3}),

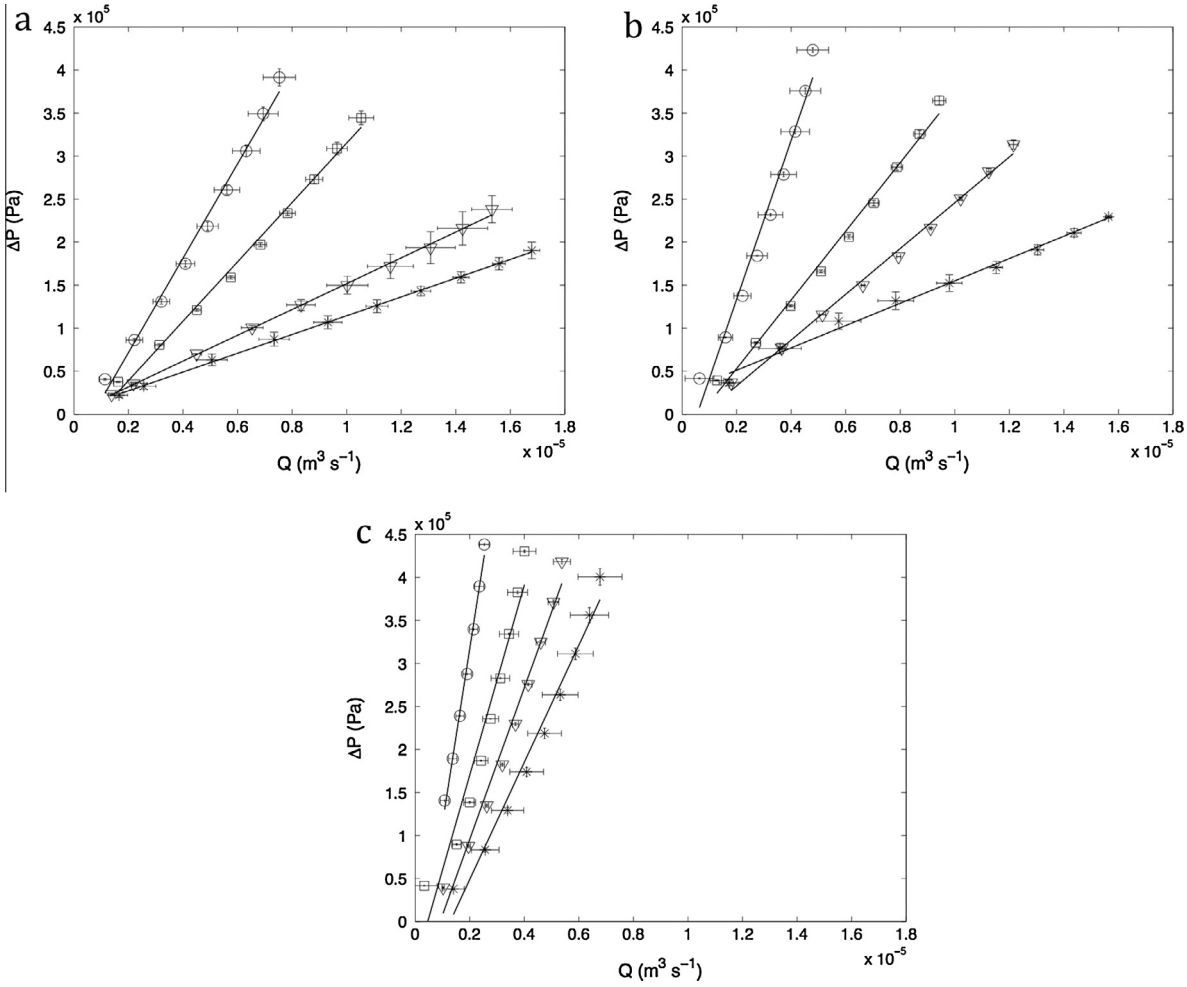

Fig. 10. Average flow rate (x-axis) – pressure drop (y-axis) data at the starting bed bulk density of (a) 360 kg m^{-3} (b) 400 kg m^{-3} and (c) 480 kg m^{-3}; particle size distributions A (○), B (□), C (▽) and D (∗) The solid lines represent the best-fit lines ($R^2 > 0.97$ for all cases) from the data to Eq. (1), rearranged to make Q the independent variable. The error bars represent the standard deviation of the measurement on three independent beds of each particle size distribution.

Table 2
Experimental permeability estimated from Eq. (1) and the collected flow rate – pressure drop data. The values represent the average of the measurements performed on three independent samples of each particle size distribution ± the standard deviation.

Particle size distribution	ρ_{bulk} 360 kg m^{-3}	ρ_{bulk} 400 kg m^{-3}	ρ_{bulk} 480 kg m^{-3}
A	$7.65 \pm 0.82 \times 10^{-14(a,b)}$	$4.94 \pm 0.32 \times 10^{-14(c)}$	$2.59 \pm 0.25 \times 10^{-14(d)}$
B	$1.37 \pm 0.08 \times 10^{-13(e)}$	$1.18 \pm 0.09 \times 10^{-13(e)}$	$4.87 \pm 0.09 \times 10^{-14(c)}$
C	$2.39 \pm 0.49 \times 10^{-13(f)}$	$1.93 \pm 0.10 \times 10^{-13(f)}$	$6.44 \pm 0.35 \times 10^{-14(b)}$
D	$3.36 \pm 0.58 \times 10^{-13(h)}$	$4.38 \pm 0.40 \times 10^{-13(g)}$	$8.95 \pm 0.75 \times 10^{-14(a)}$

Different letters indicate significant differences for different particle size distributions and ρ_{bulk}.

achieved by adding 2.30 extra grams to the bed, caused the permeability of the bed to decrease between 3 and 4-fold. Particle size distribution has a much bigger effect on permeability when the initial bed bulk density was 360 and 400 kg m^{-3} than for the case when the initial bed bulk density was 480 kg m^{-3}. For initial bed bulk density of 360 kg m^{-3} the permeability of the coarse particle size distribution (D) is 4.4 times that of the fine one (A), whereas this ratio is reduced to 3.4 when it comes to initial bed bulk density of 480 kg m^{-3}. This becomes more obvious if the permeability values are plotted against $d_{[3,2]}$ (Fig. 11). It is observed that the permeability-$d_{[3,2]}$ dependency is significantly different in the case of initial bed bulk density of 480 kg m^{-3} and this difference becomes more obvious the bigger the particle size. It has to be noted that, as previously shown in Fig. 7, higher forces (especially for coarser distributions) were applied to obtain an initial bed bulk density of 480 kg m^{-3}, as compared to the lower density beds. Therefore the different dependency may be explained due to a more dramatic modification of the initial packing structure of the bed caused by such forces.

4.5. Calculation of intrinsic density, open, closed and bed bulk porosity

The intrinsic density for coffee particles was found to be 1337 ± 2.31 kg m^{-3}. Fig. 12a shows the cumulative volume of mercury intruded into the total pore space (penetrometer pore space + pore space of the particles) during porosimetry experiments. The vertical line delimits the border between the outer (right region, $d_{pore} \geqslant 40$ μm) and particle pore space (left region, $d_{pore} < 40$ μm). Open porosity was found to lie between 0.37 and 0.47 (Fig. 12b) without a clear tendency; the relatively high error

in open porosity measurement can be attributed to the intrinsic variability of the microstructure of natural products. Closed porosity increased with particle size from 0.07 to 0.14 (Fig. 12b) and we infer that this is due to the larger particles maintaining greater proportion of intact cell pockets. The total porosity (between 0.50 and 0.57) of the particle size distributions was obtained by adding both the calculated open and closed porosity (Fig. 12b). The average total porosity of the four particle size distributions, 0.53, was taken for the calculation of $\rho_{particle}$ with Eq. (6b). Estimations of the bed bulk porosity were obtained from Eq. (6a) and were subsequently corrected according to Eq. (9) to account for bed consolidation. Fig. 13 shows the corresponding estimates for the bed bulk porosity accounting for consolidation. All the values were found to be lie between 0.12 and 0.33, being far below 0.36, the minimum empirical porosity that can be achieved in random close packed bed of mono-sized spheres (Scott, 1960).

It is also unclear to what degree swelling of the cellulose matrix occurs in a pressurised packed bed, which has undergone strong mechanical and hydrodynamic consolidation (c.f. Figs. 6b and 7). We therefore use the bed bulk porosity values calculated from dry grains and corrected to account for consolidation as input parameters for Model 1 and Model 2 and test how well these models predict the experimental permeability data.

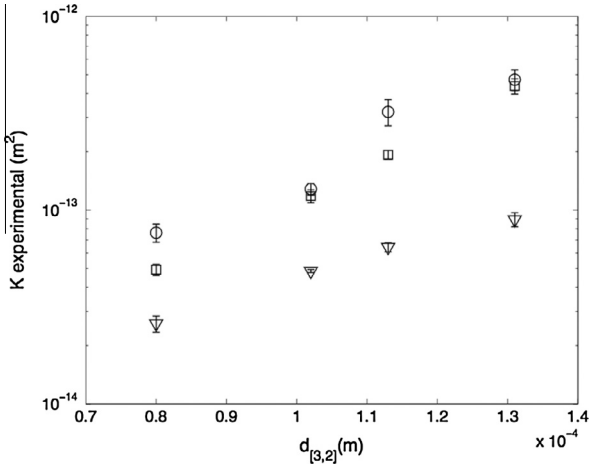

Fig. 11. Dependency of experimental permeability (logarithmic *y*-axis) on $d_{[3,2]}$ (*x*-axis) for the starting bed bulk density of 360 (○), 400 (□), and 480 kg m^{-3} (▽). The error bars represent the standard deviation of the permeability as measured in three independent samples of each particle size distribution accounting also for error propagation.

4.6. Comparison of Model 1, Model 2 predictions against experimental data

The computation of bed permeability with Model 1 and the measured bed parameters (i.e. Fig. 13 and Table 1) shows that there is a strong disagreement between model predictions and experimental data (Fig. 14a). The error, normalised to the experimental data, increases with particle size (31% for particle size distribution A as opposed to 521% for particle size distribution D). The disagreement, which in the case of coarse particles is comparable to that reported by Macdonald et al. (1979), is not surprising, as the particle size distributions are bimodal. Furthermore it is unlikely that axial compression and hydrodynamic consolidation of the bed can be taken into account just as a mere decrease in bed bulk porosity. When the dependency of tortuosity on porosity is considered (Model 2 with $n = 0.5$, as found by Dias et al. (2006) for a random close packed bed of bi-sized spheres), Fig. 14b shows that the prediction is still poor but there is a notable effect on coarser particle size distributions (relative error of 338% for particle size distribution D as opposed to 521% found with Model 1).

Therefore the tortuosity exponent, n, in Model 2 was varied in an attempt to fit to the experimental data with a single value of '*n*' applied to each distribution over the range of initial bed bulk densities. Model 2 was transformed into a polynomial of ε_{bed} whose exponents included the parameter '*n*'. This parameter was fitted with least error against the experimental data presented in Fig. 13 and Tables 1 and 2. The fitted parameter ($R^2 > 0.81$–0.98) was found to lie between 0.27 and 1.01 and increased with particle size distribution (Fig. 15). As discussed in Section 4.3 and 4.4, and taking into account that '*n*' accounts for bed packing structure, the values are consistent with the fact that higher axial forces were applied to coarser particle size distributions to pack the beds (Fig. 7) and thus the original packing structure (i.e. tortuosity, particle shape) may be more affected than in the case of fine particle size distributions. The Kozeny–Carman pre-factors (c.f. 180 in Eq. (5a)) calculated as shown in Section 2 but with fitted '*n*' parameter were between 196 and 1330; they are in good agreement with the reported values for other consolidated beds (Macdonald et al., 1979) and beds made up of other non-spherical packing materials (Nemec and Levec, 2005).

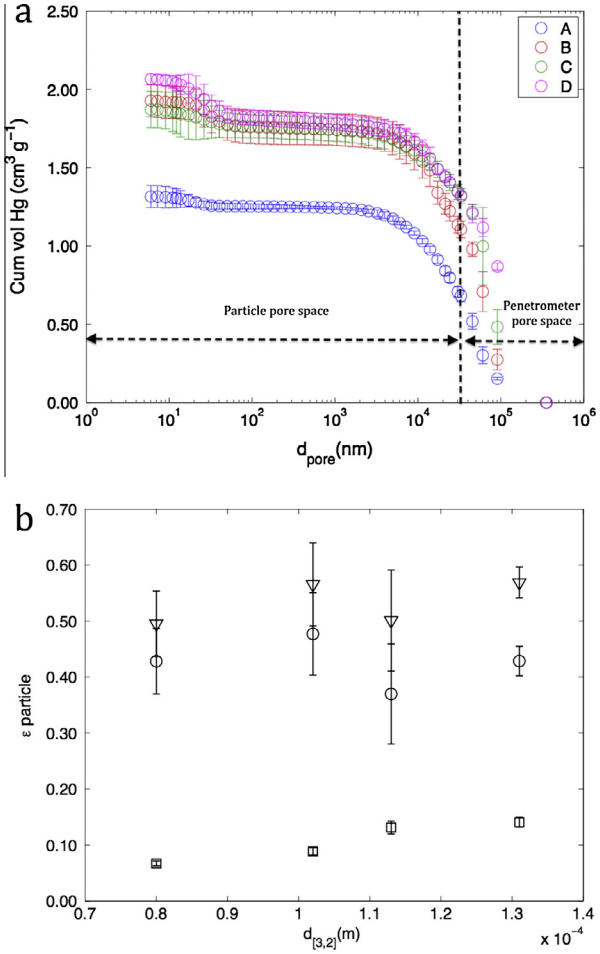

Fig. 12. (a) Cumulative specific volume of mercury (*y*-axis) for particle size distributions A–D, as a function of pore size (*x*-axis). The vertical line (d_{pore} ~ 40 μm) delimits the particle and penetrometer pore space; (b) porosity of coffee particles (*y*-axis) as a function of $d_{[3,2]}$ (*x*-axis); open porosity (○), closed porosity (□) and total porosity (▽). The error bars represent the standard deviation of the porosity as measured in three independent samples of each particle size distribution accounting also for error propagation.

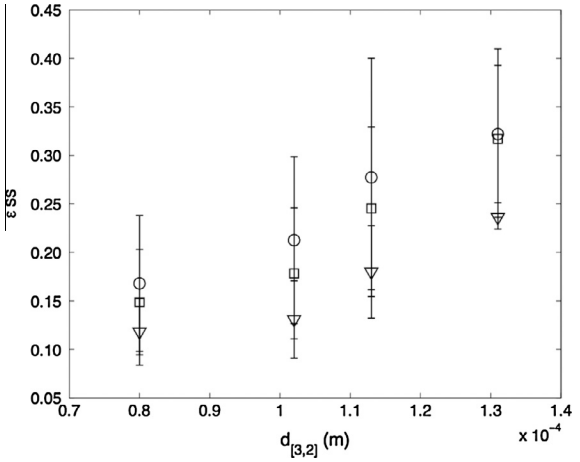

Fig. 13. Steady-state bed bulk porosity (y-axis) as a function of $d_{[3,2]}$ (x-axis) at the starting bed bulk density of 360 (○) 400 (□) and 480 (▽) kg m^{-3}. Steady-state porosity was calculated from Eq. (6a) and corrected with Eq. (9) to account for bed consolidation. The error bars represent the standard deviation of the bed bulk porosity as measured in three independent samples of each particle size distribution accounting also for error propagation.

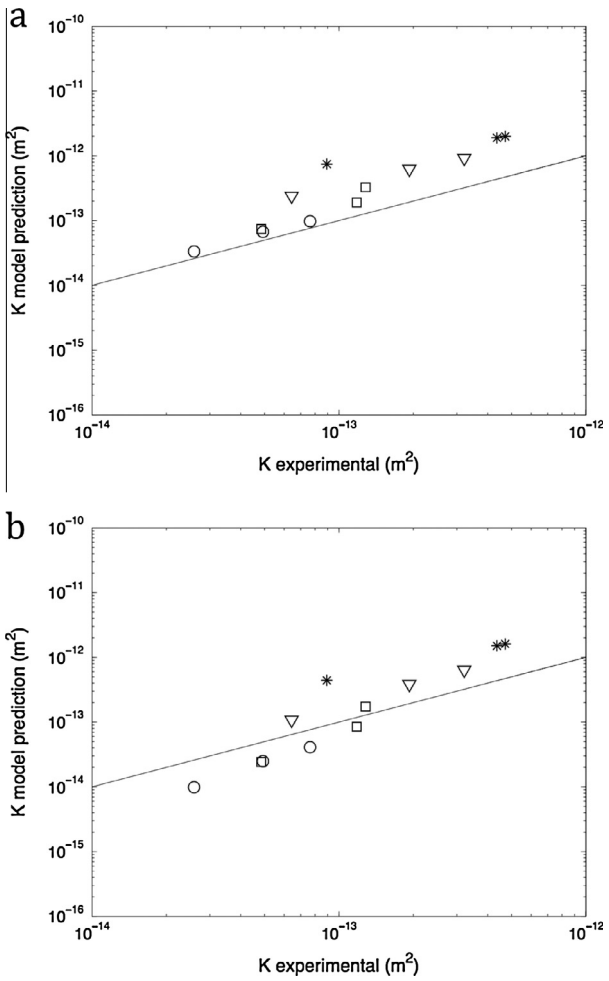

Fig. 14. Comparison between the experimental permeability for particle size distribution A (○), B (□), C (▽) and D (∗) at the starting bed bulk density of 360, 400 and 480 kg m^{-3} (x-axis) and the theoretical permeability (y-axis) as predicted with (a) Model 1 (i.e. Kozeny–Carman equation); (b) Model 2 with $n = 0.5$. The solid line represents $y = x$.

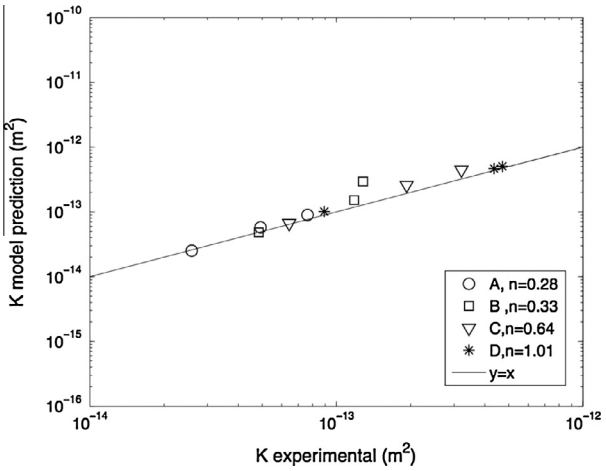

Fig. 15. Comparison between the experimental permeability for particle size distribution A–D at the starting bed bulk density of 360, 400 and 480 kg m^{-3} (x-axis) and the theoretical permeability (y-axis), as predicted with Model 2 and the fitted values of the parameter n for each particle size distribution.

5. Conclusions

The permeability of coffee packed beds in steady-state was estimated from experimental flow rate–pressure drop data which was successfully fitted to Darcy's law. Permeability was found to be very sensitive to particle size distribution measured dry and bed bulk density (i.e. bed bulk porosity); the influence of permeability on mass transfer, and thus on under or over-extraction, needs to be considered when analysing the effect of process/formulation parameters on brew quality.

Disagreement between the experimental and theoretical permeability values, obtained using the Kozeny–Carman equation (Model 1), although improved with Model 2 ($n = 0.5$), suggests that consolidation of the bed appeared to have a larger effect on the packing structure (i.e. bed tortuosity) than a mere decrease in bed bulk porosity that was accounted for in the analysis. In a further attempt to improve the model based on dry measured size distribution, the exponential parameter, n, of the tortuosity function in Model 2 was fitted. The fitted values increased the coarser the particle size distribution; this variation of tortuosity is consistent with the fact that higher forces were applied to pack coarser particle size distributions. Kozeny–Carman pre-factors (c.f. 180 in Eq. (5a)) calculated with fitted parameter were between 196 and 1330, which compared well to values reported for other consolidated and non-spherical packing materials beds. Further work to assess the potential influence of swelling of the cellulose matrix on the porosity of coffee packed beds is under progress; this may provide a separate route to improve the model. As noted earlier, alternative methodologies to characterise particle size distribution (e.g. wet dispersion measurements as opposed to the dry dispersion used in this work) may result in different particle size distributions; however our preliminary wet measurements show that $d_{[3,2]}$ values resulting from wet measurements significantly underestimate permeability.

A transient regime was observed to last over the first 60–80 s of the application of flow. Since a typical espresso extraction occurs within the time scale of this transient, we are developing the method to measure the permeability changes during the transient regime.

This study constitutes the first step of a new approach into coffee technology. It is hoped in time that predictions about preparation times and required pressures can be made with more information than empirical evidence.

Acknowledgements

The authors would like to acknowledge Mondelèz International for sponsorship and permission to publish this work, Dr. Mark Norton (Mondelèz International) for his help with the design of the extraction rig, Gael Le Barzic (Mondelèz International), for his help and assistance with the performance and interpretation of the statistical test, and the EPSRC for financial support via the Formulation Engineering Doctorate program. Dr. James Bowen (University of Birmingham UK) is also acknowledged for fruitful discussions on the pycnometry and porosity measurements.

The Micromeritics AccuPyc II 1340 Helium Pycnometer, Micromeritics AutoPore IV Mercury Porosimeter, Sympatec QICPIC Particle Size analyser, and Z030 mechanical tester used in this research were obtained through Birmingham Science City: Innovative Uses for Advanced Materials in the Modern World (West Midlands Centre for Advanced Materials Project 2), with support from Advantage West Midlands (AWM) and part funded by the European Regional Development Fund (ERDF).

References

Andueza, S., Maeztu, L., Dean, B., de Peña, M.P., Bello, J., Cid, C., 2002. Influence of water pressure on the final quality of arabica espresso coffee. Application of multivariate analysis. J. Agric. Food Chem. 50 (25), 7426–7431. http://dx.doi.org/10.1021/jf0206623.

Andueza, S., Maeztu, L., Pascual, L., Ibáñez, C., de Peña, M.P., Cid, C., 2003. Influence of extraction temperature on the final quality of espresso coffee. J. Sci. Food Agric. 83, 240–248. http://dx.doi.org/10.1002/jsfa.1304.

Andueza, S., Vila, A.M., de Peña, M.P., Cid, C., 2007. Influence of coffee/water ratio on the final quality of espresso coffee. J. Sci. Food Agric. 592, 586–592. http://dx.doi.org/10.1002/jsfa.

Bear, J., 1988. Dynamics of Fluids in Porous Media, second ed. Dover publications, INC, New York.

Caprioli, G., Cortese, M., Cristalli, G., Maggi, F., Odello, L., Ricciutelli, M., et al., 2012. Optimization of espresso machine parameters through the analysis of coffee odorants by HS-SPME-GC/MS. Food Chem. 135 (3), 1127–1133. http://dx.doi.org/10.1016/j.foodchem.2012.06.024.

Clarke, R.J., 2001. Technology III: instant coffee. In: Clarke, R.J., Vitzthum, O.G. (Eds.), Coffee Recent Developments, first ed. Blackwell Science, Oxford, pp. 125–137.

Di Felice, R., Gibilaro, L.G., 2004. Wall effects for the pressure drop in fixed beds. Chem. Eng. Sci. 59 (14), 3037–3040. http://dx.doi.org/10.1016/j.ces.2004.03.030.

Dias, R., Teixeira, J., Mota, M., Yelshin, A., 2006. Tortuosity variation in a low density binary particulate bed. Sep. Purif. Technol. 51 (2), 180–184. http://dx.doi.org/10.1016/j.seppur.2006.01.010.

Endo, Y., Chen, D.-R., Pui, D.Y.H., 2002. Theoretical consideration of permeation resistance of fluid through a particle packed layer. Powder Technol. 124 (1–2), 119–126. http://dx.doi.org/10.1016/S0032-5910(01)00479-X.

Gianino, C., 2007. Experimental analysis of the Italian coffee pot "moka". Am. J. Phys. 75 (1), 43. http://dx.doi.org/10.1119/1.2358157.

Giesche, H., 2006. Mercury porosimetry: a general (practical) overview. Part. Part. Syst. Charact. 23 (1), 9–19. http://dx.doi.org/10.1002/ppsc.200601009.

Gloess, A.N., Schönbächler, B., Klopprogge, B., D'Ambrosio, L., Chatelain, K., Bongartz, A., et al., 2013. Comparison of nine common coffee extraction methods: instrumental and sensory analysis. Eur. Food Res. Technol. 236 (4), 607–627. http://dx.doi.org/10.1007/s00217-013-1917-.

Hekmat, D., Mornhinweg, R., Bloch, G., Sun, Y., Jeanty, P., Neubert, M., Weuster-Botz, D., 2011. Macroscopic investigation of the transient hydrodynamic memory behavior of preparative packed chromatography beds. J. Chromatogr. A 1218 (7), 944–950. http://dx.doi.org/10.1016/j.chroma.2010.12.092.

International Coffee Organization, 2013. <http://www.ico.org> (Retrieved 20.09.13).

Joseph, J., Siva Kumar Gunda, N., Mitra, S.K., 2013. On-chip porous media: porosity and permeability measurements. Chem. Eng. Sci. 99, 274–283. http://dx.doi.org/10.1016/j.ces.2013.05.065.

King, W.D., 2008. The physics of a stove-top espresso machine. Am. J. Phys. 76 (6), 558. http://dx.doi.org/10.1119/1.2870524.

Lanfrey, P.-Y., Kuzeljevic, Z.V., Dudukovic, M.P., 2010. Tortuosity model for fixed beds randomly packed with identical particles. Chem. Eng. Sci. 65 (5), 1891–1896. http://dx.doi.org/10.1016/j.ces.2009.11.011.

Lindinger, C., Labbe, D., Pollien, P., Rytz, A., Juillerat, M.A., Yeretzian, C., Blank, I., 2008. When machine tastes coffee: instrumental approach to predict the sensory profile of espresso coffee. Anal. Chem. 80 (5), 1574–1581. http://dx.doi.org/10.1021/ac702196z.

Macdonald, I.F., El-Sayed, M.S., Mow, K., Dullien, F.A.L., 1979. Flow through porous media-the Ergun equation revisited. Ind. Eng. Chem. Fundam. 18 (3), 199–208. http://dx.doi.org/10.1021/i160071a001.

Maeztu, L., Andueza, S., Ibañez, C., de Peña, M.P., Bello, J., Cid, C., 2001. Multivariate methods for characterization and classification of espresso coffees from different botanical varieties and types of roast by foam, taste, and mouthfeel. J. Agric. Food Chem. 49 (10), 4743–4747. http://dx.doi.org/10.1021/jf010314l.

Mateus, M., Rouvet, M., 2007. Interactions of water with roasted and ground coffee in the wetting process investigated by a combination of physical determinations. J. Agric. Food Chem. 55, 2979–2984.

Navarini, L., Nobile, E., Pinto, F., Scheri, A., Suggi-liverani, F., 2009. Experimental investigation of steam pressure coffee extraction in a stove-top coffee maker. Appl. Therm. Eng. 29 (5–6), 998–1004. http://dx.doi.org/10.1016/j.applthermaleng.2008.05.014.

Nemec, D., Levec, J., 2005. Flow through packed bed reactors: 1. Single-phase flow. Chem. Eng. Sci. 60 (24), 6947–6957. http://dx.doi.org/10.1016/j.ces.2005.05.068.

Parenti, A., Guerrini, L., Masella, P., Spinelli, S., Calamai, L., Spugnoli, P., 2014. Comparison of espresso coffee brewing techniques. J. Food Eng. 121, 112–117. http://dx.doi.org/10.1016/j.jfoodeng.2013.08.031.

Petracco, M., 2001. Technology IV: beverage preparation: brewing trends for the new millennium. In: Clarke, R.J., Vitzthum, O.G. (Eds.), Coffee Recent Developments, first ed. Blackwell Science, Oxford, pp. 140–162.

Petracco, M., 2005. Percolation. In: Viani, R., Illy, A. (Eds.), Espresso Coffee. The Science of Quality, second ed. Elsevier Academic Press, San Diego, pp. 259–280.

Petracco, M., Liverani, F.S., 1993. Dynamics of fluid percolation through a bed of particles subject to physico-chemical evolution, and its mathematical modelization. In: ASIC (Ed.), 15th International Conference on Coffee Science, pp. 702–711.

Rhodes, M., 2008. Fluid flow through a packed bed of particles. In: Introduction to particle technology, second ed. Wiley, pp. 153–165.

Romani, S., Severini, C., Fiore, A.G., Pinnavaia, G.G., 2004. Quality of "Espresso" coffee: a study performed through Italian coffee shops. In: ASIC (Ed.), 20th International Conference on Coffee Science. Bangalore, India, pp. 521–525.

Schenker, S., Handschin, S., Frey, B., Perren, R., Escher, F., 2000. Pore structure of coffee beans affected by roasting conditions. J. Food Sci. 65 (3), 452–457. http://dx.doi.org/10.1111/j.1365-2621.2000.tb16026.x.

Scott, G.D., 1960. Packing of spheres: packing of equal spheres. Nature 188 (4754), 908–909. http://dx.doi.org/10.1038/188908a0.

Tien, C., Ramarao, B.V., 2013. Can filter cake porosity be estimated based on the Kozeny–Carman equation? Powder Technol. 237, 233–240. http://dx.doi.org/10.1016/j.powtec.2012.09.031.